Thomson-Scattering Detection of Plasma Waves Excited by Two Laser Beams

Behrouz Amini and Francis F. Chen
University of California, Los Angeles, California 90024
(Received 30 April 1984)

Electron plasma waves excited by optical mixing of two antiparallel CO_2 laser beams have been detected by ruby-laser Thomson scattering. The density resonance is confirmed by two separate methods.

PACS numbers: 52.35.Mw, 42.65.Cq, 52.40.Mj, 52.70.Kz

Excitation of plasma waves by beat-frequency mixing of laser or rf beams has been of great interest for two decades because of its possible application to plasma heating,[1-5] plasma diagnostics,[6,7] ionospheric sounding,[8] plasma lasers,[9] feedback stabilization,[10] and particle accelerators.[11] We also suggest that a localized heat source like this could be used for studies of cross-field heat transport. The growth and saturation of the plasma waves have been treated by a number of theorists,[12-16] but experimental observations are extremely limited.[17-20] In this Letter we report the first measurement of the plasma wave excited by a CO_2 laser in a long-scale-length plasma, together with a definitive verification of the density resonance. The signal-to-noise ratio is 1–2 orders of magnitude higher than in the pioneering experiment of Stansfield, Nodwell, and Meyer[17] with dye lasers.

The experimental arrangement is shown in Fig. 1. The plasma is produced by a fast theta pinch with a 4.25-μsec ringing time, a 10-cm-i.d. and 22.5-cm-long coil with a 2.5-cm gap at the midplane, and a 7.5-cm-i.d. quartz chamber. The He plasma is compressed a factor of 3 in radius and at the time of measurement is fully ionized with $T_e \simeq 30$ eV and $T_i \simeq 80$ eV. The two 50-nsec (full width at half maximum) CO_2-laser beams at $\lambda = 9.55$ μm (P-20) and 10.26 μm (R-18) are generated in the same oscillator with use of an intracavity SF_6 cell,[21] separated with a grating, and focused coaxially at the center of the plasma by lenses L2 and L1. The spot sizes are kept large to assure good beam overlap and definition; approximately rectangular, they are 1.7×2.5 and 2.5×3.4 mm^2 for the 9.6- and 10.3-μm beams, respectively. The average intensities are $\simeq 1.3 \times 10^9$ and 1.3×10^8 W/cm^2, well below the stimulated-Raman-instability threshold of $\simeq 10^{11}$ W/cm^2.

The 25-nsec (full width at half maximum), 1-J ruby-laser beam ($\lambda = 0.6943$ μm) used for diagnostics is focused by lens L3 to a 600-μm-diam spot inside the interaction region defined by the overlap of the CO_2-laser beams. The ruby light enters and leaves through midplane ports of 2×2.4 cm^2 clear

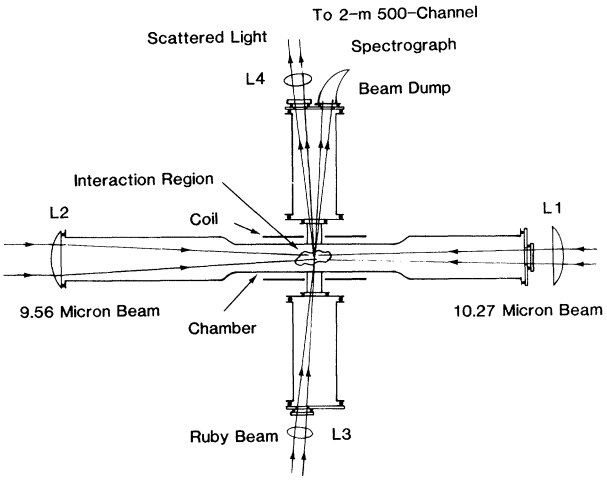

FIG. 1. Experimental arrangement.

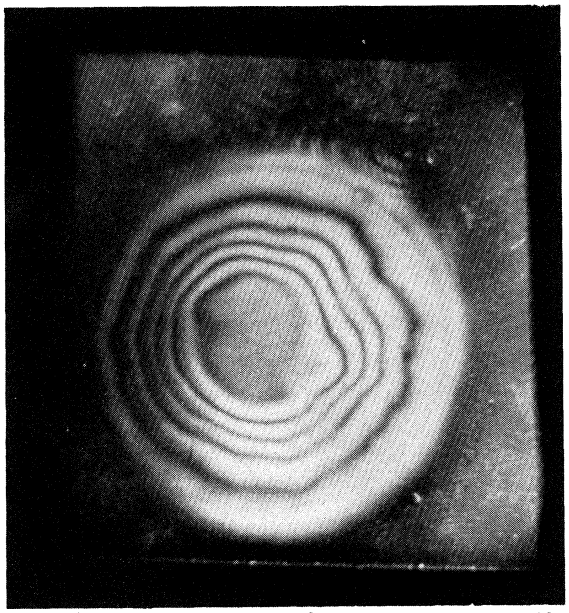

FIG. 2. End-on ruby interferogram showing uniform density and therefore no trapped magnetic field in the central region (1.3×10^{16} cm^{-3} per fringe).

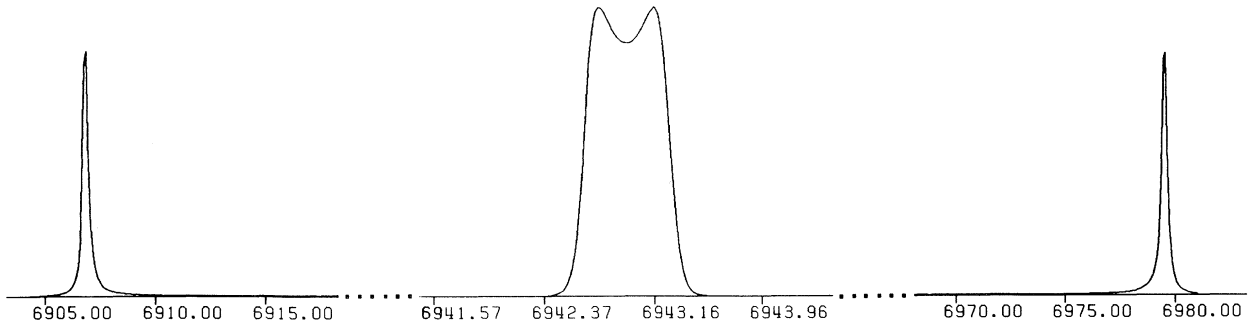

FIG. 3. Theoretical Thomson-scattering spectrum for a thermal plasma. The scale has been expanded at the center to show the ion feature.

aperture, and the scattered light is collected by lens L4, subtending an angle of 0.005 sr (1.5 times the ruby-laser divergence), and sent to a 2-m spectrograph and a 500-channel digital multichannel analyzer. Timing of the laser pulses relative to the pinch is monitored by a photodiode sensitive to the optical radiation seen through a third midplane port.

The plasma density n_0 is independently measured by Thomson scattering, as explained later, and by simultaneous end-on and side-on holographic interferometry (Fig. 2) using the same ruby laser in a different setup. This shows a radial density profile with a 5-mm-diam flat top, sufficient to cover the CO_2-laser focal spots; and the absolute density can be set equal to the resonance value of 5.0×10^{16} cm^{-3} (see later) for a period of 80–100 nsec. Electron temperature was measured by the line-to-continuum ratio of the He II 4686 Å line. Ion temperature was estimated by three methods, which agree: (1) line profile of 4686 Å, with assumption of simple convolution of Stark and Doppler broadening; (2) assuming that the kinetic energy of the ions during implosion is all converted into heat, and (3) presure balance with assumption of $\beta=1$ and use of the previous measurements of n_0 and T_e and the known coil current.

In optical mixing, beating of the two pump beams $(\omega_0, \vec{k}_0)$ at 9.6 μm and $(\omega_1, \vec{k}_1)$ at 10.3 μm forms a pattern of ponderomotive force with frequency and wave number

$$\Delta\omega=\omega_0-\omega_1, \quad \Delta\vec{k}=\vec{k}_0-\vec{k}_1; \tag{1}$$

and this drives density perturbations with $\omega=\Delta\omega$, $\vec{k}=\Delta\vec{k}$. The interaction peaks when ω matches a natural frequency of the plasma—in this case, the Bohm-Gross frequency for electron plasma waves,

$$\omega=\omega_{BG}=(\omega_p^2+3k^2v_e^2)^{1/2}, \tag{2}$$

where $\omega_p^2=4\pi n_0e^2/m$ and $v_e^2=KT_e/m$. Since the light waves satisfy

$$\omega_{0,1}^2=\omega_p^2+k_{0,1}^2c^2, \tag{3}$$

the simultaneous solution of Eqs. (1)–(3) gives ω, $\vec{k}$, $\vec{k}_0$, $\vec{k}_1$, and ω_p when ω_0, ω_1, T_e, and the angle θ between $\vec{k}_0$ and $\vec{k}_1$ are specified. In the present case of $\theta=180°$ and $\omega_0^2\simeq200\omega_p^2>>\omega_p^2$, Eqs. (1)–(3) give $|k|\simeq2|k_0|$ and $n_0=5.0\times10^{16}$ cm^{-3}. Thus the plasma wave has $\lambda\simeq5$ μm, and the resonant density is $\simeq5\times10^{16}$ cm^{-3}.

For the Thomson-scattering system, let $\vec{k}_i$ and $\vec{k}_s$ be the incident and scattered ruby-laser wave vectors, respectively, and let ϕ be the angle between them. The k-matching condition $\vec{k}_i=\vec{k}_s+\vec{k}$ then requires $\sin(\phi/2)=k/2k_i$, where $k=k_0+k_1$ is the k of the detected plasma wave. The angle ϕ is then fixed at 8.0° and is split symmetrically about the midplane (Fig. 1). The scattering parameter $\alpha=1/k\lambda_D$ in this case is 4.35, so that the scattering is in the collective regime, and one expects the observed spectrum to consist of an ion feature plus two electron wave peaks at $\omega_s=\omega_i\pm\omega_{BG}$ (Fig. 3). Only the red-shifted peak is used here because of the proximity of the blue peak to a spectral line of He.

Figure 4 shows an example of the 2-m 500-channel spectrograph output at a dispersion of 0.2 Å/channel, showing the red-shifted plasma-wave peak at a shift of 35.2 Å, or 176 channels, corresponding to the density at that time. The spectrograph slit was widened to 1000 μm to insure collection of all of the scattered light, allowing it to show above the stray-light background. The width of the peak is consistent with the density gradient, the density variation during the ruby-laser pulse, and geometrical factors. The level of the plasma satellites is above thermal; this level is unchanged if only one CO_2 beam is incident and fluctuates only 10% from shot to shot.

When optical mixing occurs, the plasma peak is greatly enhanced, as shown in Fig. 5, which is taken with a 200-μm slit width. The enhancement factor depends on the proximity of ω_{BG} to $\Delta\omega$ and reaches a maximum of about 70. The position of the peak

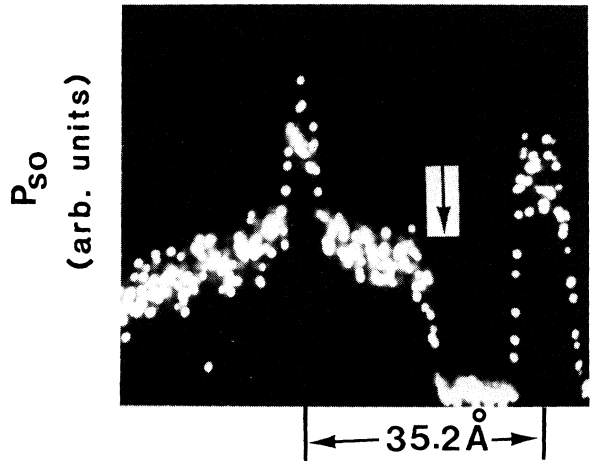

FIG. 4. Thomson-scattered spectrum in the absence of wave excitation. The portion to the right of the arrow has been attenuated to show the unshifted stray-light peak.

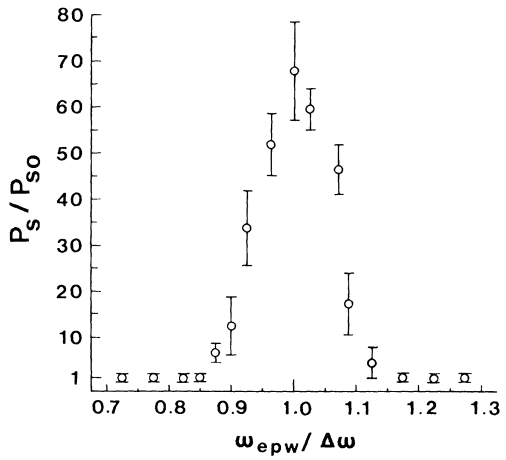

FIG. 6. Enhancement factor vs plasma-wave frequency normalized to the beat frequency between the two strongest lines in the CO_2 pumps.

can be determined within three channels, corresponding to a density uncertainty of only 1%. Thus the resonance condition $\Delta\omega = \omega_{BG}$ can be checked in a self-calibrating way. By varying the filling pressure, the resonance curve can be traced (Fig. 6). The error bars reflect the variation in height and in ω_{BG} in the shots that have been averaged to give each point. Note, however, that the plasma-wave frequency ω_{epw} is known within 1% in each shot, whether it be ω_{BG} or ω_{BG} plus a nonlinear frequency shift[22] of $\simeq \frac{1}{2}\%$. The presence of weaker lines in the CO_2- and ruby-laser beams can cause a width of $\pm 9\%$ in the curve of Fig. 6, in agreement with what is observed.

The density resonance can be demonstrated in a single shot by masking one of the pump beams into three strips. These are made to fall on a region of steep density gradient, so that each 1.7×0.5 mm^2 strip, separated from the next by 0.5 mm, falls on a different density region. When the density is adjusted so that the middle strip falls on the correct density, the scattered spectrum (Fig. 7) shows three peaks, with the highest in the middle. The density can also be adjusted so that the resonant region is on either side. The range of wavelengths in the pump waves is sufficient to cover the density variation. This technique can be used to measure density profiles on a very fine scale.

The theory of optical mixing[8,12-15] shows that the plasma-wave amplitude $\tilde{n}$ grows linearly with time until either a parametric instability occurs or the wave saturates. Rosenbluth and Liu[13] consider sat-

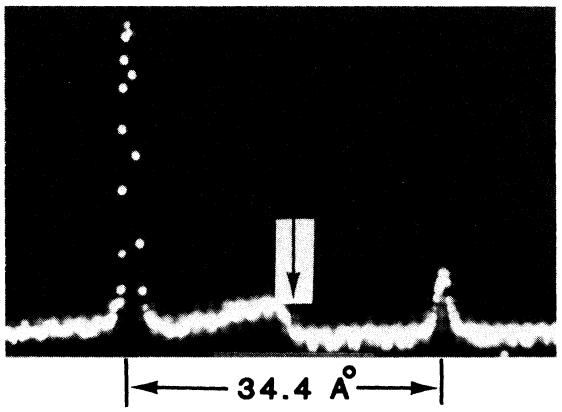

FIG. 5. Scattered spectrum in the presence of driven plasma waves. The satellite level would not be visible on this scale. Again, the right-hand portion has been artificially suppressed.

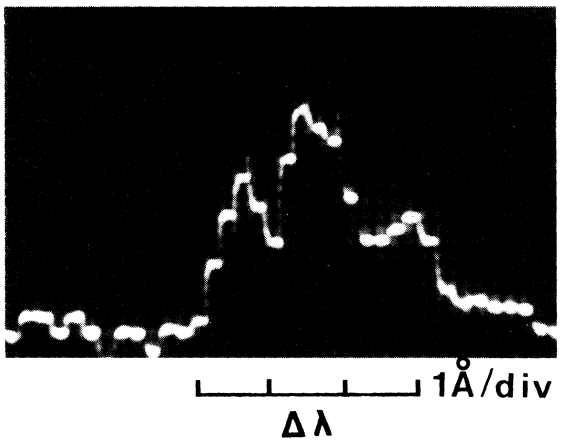

FIG. 7. Scattered spectrum with a divided pump beam where only the middle part sees the resonant density.

uration due to the relativistic increase in electron mass. However, saturation can also occur when the damping overcomes the drive. If the plasma-wave damping rate is γ_L, it is easy to show[23] that, for oppositely directed beams,

$$\tilde{n}/n_0 = (v_0 v_1 k^2/4\omega\gamma_L)(1-e^{-\gamma_L t}), \quad (4)$$

where $v_j = eE_j/m\omega_j$ are the quiver velocities of the two beams. In this experiment, γ_L is primarily due to Landau damping and is $\simeq 1.2\times 10^{10}$ sec^{-1}. Thus, for our pump intensities, $\tilde{n}/n_0$ saturates at 0.6% in $\simeq 0.1$ nsec, below the level of $\simeq 1.6\%$ expected from relativistic effects.

In this Letter we have shown (1) that collective Thomson scattering can give a precise measurement of the plasma-wave frequency, (2) that optical mixing of antiparallel laser beams drives up the plasma waves in a manner consistent with theory, (3) that the resonance condition $\Delta\omega = \omega_{BG}$ must be met before this happens, and (4) that optical mixing with masked beams offers a way to measure steep density gradients.

This work was supported by the National Science Foundation through Grants No. ENG-75-16610, and No. ECS-81-20933, 80-03558, and 83-10972, by the U.S. Department of Energy under Contract No. DE-AS08-81-DP40163, and by the Lawrence Livermore Laboratory, Order No. 3446905.

[1]B. I. Cohen, A. N. Kaufman, and K. M. Watson, Phys. Rev. Lett. **29**, 581 (1972).

[2]A. N. Kaufman and B. I. Cohen, Phys. Rev. Lett. **30**, 1306 (1973).

[3]B. I. Cohen, M. A. Mostrom, D. R. Nicholson, A. N. Kaufman, and C. E. Max, Phys. Fluids **18**, 470 (1975).

[4]V. Fuchs, C. R. Neufeld, J. Teichmann, and A. G. Engelhardt, Phys. Rev. Lett. **31**, 1110 (1973).

[5]J. E. Willett and B. Maraghechi, Plasma Phys. **18**, 829 (1976).

[6]R. Cano, I. Fidone, and B. Zanfagna, Phys. Fluids **14**, 811 (1971).

[7]E. S. Weibel, Phys. Fluids **19**, 1237 (1976).

[8]G. Weyl, Phys. Fluids **13**, 1802 (1970).

[9]R. D. Milroy, C. E. Capjack, and C. R. James, Plasma Phys. **19**, 989 (1977).

[10]F. F. Chen, in *Feedback and Dynamic Control of Plasmas—1970,* edited by T. K. Chu and H. W. Hendel, AIP Conference Proceedings No. 1 (American Institute of Physics, New York, 1970), p. 33.

[11]T. Katsouleas and J. M. Dawson, Phys. Rev. Lett. **51**, 392 (1983).

[12]N. M. Kroll, A. Ron, and N. Rostoker, Phys. Rev. Lett. **13**, 83 (1964).

[13]M. N. Rosenbluth and C. S. Liu, Phys. Rev. Lett. **29**, 701 (1972).

[14]P. S. Lee, Y. C. Lee, C. T. Chang, and D. S. Chuu, Phys. Rev. Lett. **30**, 538 (1973).

[15]G. Schmidt, Phys. Fluids **16**, 1676 (1973).

[16]E. S. Weibel, Phys. Rev. Lett. **37**, 1619 (1976).

[17]B. L. Stansfield, R. Nodwell, and J. Meyer, Phys. Rev. Lett. **26**, 1219 (1971).

[18]J. Meyer, Phys. Rev. A **6**, 2291 (1972).

[19]G. G. Albach and J. Meyer, Phys. Rev. Lett. **34**, 926 (1975).

[20]C. Joshi, C. E. Clayton, and F. F. Chen, Phys. Rev. Lett. **48**, 874 (1982).

[21]C. Joshi, C. E. Clayton, and F. F. Chen, University of California, Los Angeles, Report No. UCLA PPG-537, 1981 (unpublished).

[22]A. Lee and G. Pocobelli, Phys. Fluids **15**, 2351 (1972).

[23]B. Amini and F. F. Chen, University of California, Los Angeles, Report No. UCLA PPG-746, 1983 (unpublished).

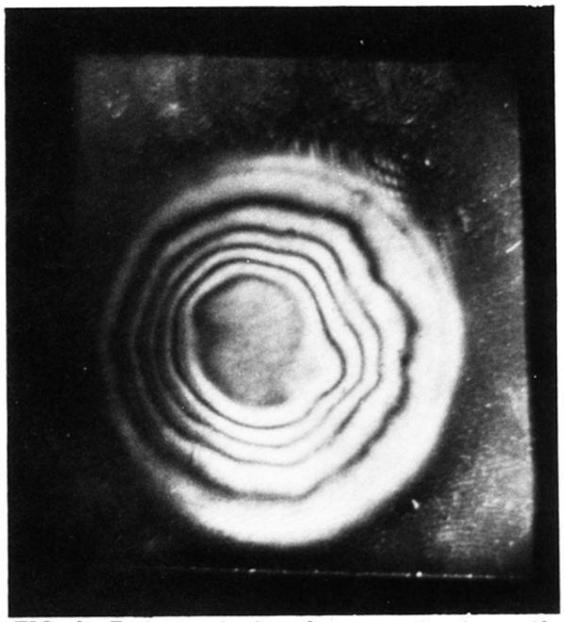

FIG. 2. End-on ruby interferogram showing uniform density and therefore no trapped magnetic field in the central region (1.3×10^{16} cm^{-3} per fringe).

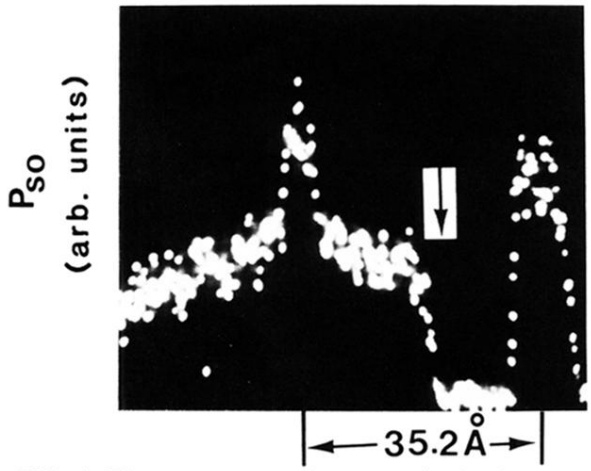

FIG. 4. Thomson-scattered spectrum in the absence of wave excitation. The portion to the right of the arrow has been attenuated to show the unshifted stray-light peak.

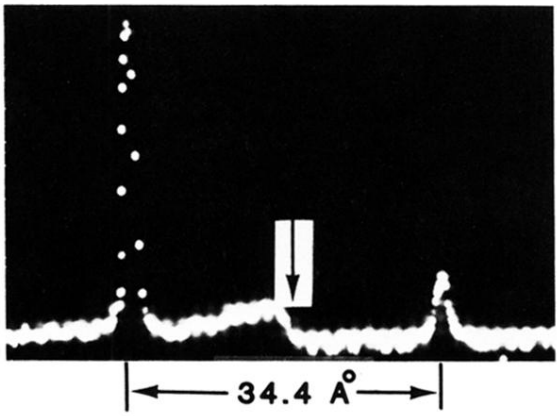

FIG. 5. Scattered spectrum in the presence of driven plasma waves. The satellite level would not be visible on this scale. Again, the right-hand portion has been artifically suppressed.

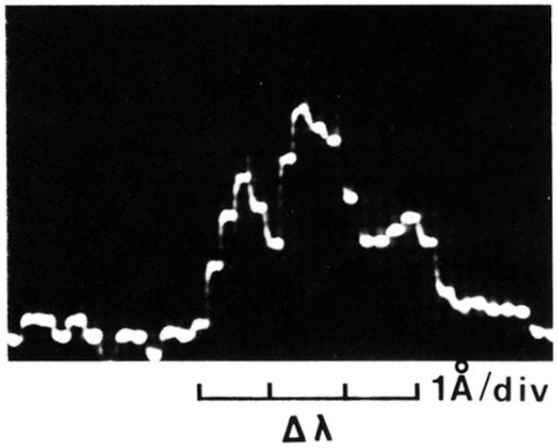

FIG. 7. Scattered spectrum with a divided pump beam where only the middle part sees the resonant density.